A spatial model for rare binary events

July 22, 2016

1 Introduction

The goal in binary regression is to relate a latent variable to a response using a link function. Two common examples of binary regression include logistic regression and probit regression. The link functions for logistic and probit regression are symmetric, so they may not be well-suited for asymmetric data. An asymmetric alternative to these link functions is the complementary log-log (cloglog) link function. More recently, Wang and Dey (2010) introduced the generalized extreme value (GEV) link function for rare binary data (a review is given in Appendix A.1). The GEV link function introduces a new shape parameter to the link function that controls the degree of asymmetry. The cloglog link is a special case of the GEV link function when the shape parameter is 0. Although this link was selected due to its ability to handle asymmetry, the GEV distribution is one of the primary distributions used for modeling extremes. Because extreme events are rare, it is therefore reasonable to use similar methods when analyzing rare binary data.

Spatial logistic and probit models commonly employ a hierarchical model assuming a latenst spatial process citation. In the hierarchical framework, spatial dependence is typically modeled with an underlying latent Gaussian process, and conditioned on this process, observations are independent. However, if the latent variable is assumed to follow a GEV marginally, then a Gaussian process may not be appropriate to describe the dependence due to the fact that Gaussian processes do not demonstrate asymptotic dependence, except in the case of perfect dependence.

We propose using a latent max-stable process (de Haan, 1984) because it allows for asymptotic dependence. The max-stable process arises as the limit of the location-wise maximum of infinitely many spatial processes. Max-stable processes are extremely flexible, but are often challenging to work with in high di-

mensions (Wadsworth and Tawn, 2014; Thibaud and Opitz, 2015). To address this challenge, methods have been proposed that implement composite likelihood techniques for max-stable processes (Padoan et al., 2010; Genton et al., 2011; Huser and Davison, 2014). As an alternative to these composite approaches, Reich and Shaby (2012) present a hierarchical model that implements a low-rank representation for a max-stable process. Although composite likelihoods have been used to model binary spatial data (Heagerty and Lele, 1998), we chose to use the low-rank representation of a max-stable process given by Reich and Shaby (2012).

Paragraph outlining the structure of the paper

2 Spatial dependence for binary regression

Let $Y(\mathbf{s})$ be the binary response at spatial location $\mathbf{s}$ in a spatial domain of interest $\mathcal{D} \in \mathcal{R}^2$. We assume $Y(\mathbf{s}) = I[Z(\mathbf{s}) > 0]$ where $Z(\mathbf{s}) = [1 - \xi\frac{\mathbf{X}(\mathbf{s})\boldsymbol{\beta}}{\sigma}]^{1/\xi}$ is a latent continuous max-stable process with unit Fréchet margins, $\mathbf{X}(\mathbf{s})$ is a p vector of spatial covariates at site $\mathbf{s}$, $\boldsymbol{\beta}$ is a p-vector of regression coefficients, and we set $\sigma = 1$ for identifiability. If $\mathbf{X}^\top(\mathbf{s})\boldsymbol{\beta} = \mu$ for all $\mathbf{s}$, then P$(Y = 1)$ is the same for all observations but we have two parameters to estimate. So when there are no covariates, we fix $\xi = 0$. Although $\boldsymbol{\beta}$ and ξ could be permitted to vary across space, we assume that they are constant across $\mathcal{D}$. At spatial location $\mathbf{s}$, the marginal distribution is $P[Y(\mathbf{s}) = 1] = 1 - \exp\left[-\frac{1}{z(\mathbf{s})}\right]$. This is the same as the marginal distribution given by Wang and Dey (2010).

For a finite collection of locations $\mathbf{s}_1, \ldots, \mathbf{s}_n$, denote the vector of observations $\mathbf{Y} = [Y(\mathbf{s}_1), \ldots, Y(\mathbf{s}_n)]^T$. The spatial dependence of $\mathbf{Y}$ is determined by the joint distribution of $\mathbf{Z} = [Z(\mathbf{s}_1), \ldots, Z(\mathbf{s}_n)]^T$ which is computationally challenging to obtain. Therefore, to incorporate spatial dependence into the model, we consider the hierarchical representation of the process proposed in Reich and Shaby (2012). Consider a set of $A_1, \ldots, A_L \overset{iid}{\sim}$ Positive Stable(α) random effects associated with spatial knots $\mathbf{v}_1, \ldots, \mathbf{v}_L$. The hierarchical

model is given by

$$\mathbf{Z}|A_1,\ldots,A_L \overset{indep}{\sim} \text{GEV}[\theta(\mathbf{s}),\alpha\theta(\mathbf{s}),\alpha] \quad \text{and} \quad A_l \overset{iid}{\sim} \text{PS}(\alpha) \tag{1}$$

where $\theta(\mathbf{s}) = \left[\sum_{l=1}^{L} A_l w_l(\mathbf{s})^{1/\alpha}\right]^{\alpha}$, $w_l(\mathbf{s}_i)$ are a set of L weights that vary smoothly across space and determine the spatial dependence structure, and $\alpha \in (0,1)$ determines the strength of dependence, with α near zero giving strong dependence and $\alpha = 1$ giving joint independence.

Because the latent $\mathbf{Z}$ are independent given the random effects, the binary responses are also conditionally independent. This leads to the tractible likelihood

$$Y_i|A_l,\ldots,A_L \overset{indep}{\sim} \text{Bern}[\pi(\mathbf{s}_i)] \tag{2}$$

where

$$\pi(\mathbf{s}_i) = 1 - \exp\left\{-\sum_{l=1}^{L} A_l \left(\frac{w_l(\mathbf{s}_i)}{Z(\mathbf{s}_i)}\right)^{1/\alpha}\right\}, \tag{3}$$

and $Z(\mathbf{s}) = [1 - \xi\mathbf{X}(\mathbf{s})\boldsymbol{\beta}]^{1/\xi}$ as before.

Many weight functions are possible, but the weights must be constrained so that $\sum_{l=1}^{L} w_l(\mathbf{s}_i) = 1$ for all $i = 1,\ldots,n$ to preserve the marginal GEV distribution. For example, Reich and Shaby (2012) take the weights to be scaled Gaussian kernels with knots $\mathbf{v}_l$,

$$w_l(\mathbf{s}_i) = \frac{\exp\left[-0.5\left(||\mathbf{s}_i - \mathbf{v}_l||/\rho\right)^2\right]}{\sum_{j=1}^{L}\exp\left[-0.5\left(||\mathbf{s}_i - \mathbf{v}_j||/\rho\right)^2\right]} \tag{4}$$

where $||\mathbf{s}_i - \mathbf{v}_l||$ is the distance between site $\mathbf{s}_i$ and knot $\mathbf{v}_l$, and the kernel bandwidth $\rho > 0$ determines the spatial range of the dependence, with large ρ giving long-range dependence and vice versa.

After marginalizing out the positive stable random effects, the joint likelihood of $\mathbf{Z}$ is given by

$$G(\mathbf{z}) = \exp\left\{-\sum_{l=1}^{L}\left[\sum_{i=1}^{n}\left(\frac{w_l(\mathbf{s}_i)}{z(\mathbf{s}_i)}\right)^{1/\alpha}\right]^{\alpha}\right\}, \tag{5}$$

where $G(\cdot)$ is the CDF of a multivariate GEV distribution. This is a special case of the multivariate GEV distribution with asymmetric Laplace dependence function (Tawn, 1990).

3 Joint distribution

We give an exact expression in the case where there are only two spatial locations which is useful for constructing a pairwise composite likelihood (Padoan et al., 2010) and studying spatial dependence. When $n = 2$, the probability mass function is given by

$$\mathrm{P}[Y(\mathbf{s}_i), Y(\mathbf{s}_j)] = \begin{cases} \varphi(\mathbf{z}) & Y(\mathbf{s}_i) = 0, Y(\mathbf{s}_j) = 0 \\ \exp\left\{-\dfrac{1}{z(\mathbf{s}_i)}\right\} - \varphi(\mathbf{z}), & Y(\mathbf{s}_i) = 1, Y(\mathbf{s}_j) = 0 \\ 1 - \exp\left\{-\dfrac{1}{z(\mathbf{s}_i)}\right\} - \exp\left\{-\dfrac{1}{z(\mathbf{s}_j)}\right\} + \varphi(\mathbf{z}), & Y(\mathbf{s}_i) = 1, Y(\mathbf{s}_j) = 1 \end{cases} \tag{6}$$

where $\varphi(\mathbf{z}) = \exp\left\{-\sum_{l=1}^{L}\left[\left(\frac{w_l(\mathbf{s}_i)}{z(\mathbf{s}_i)}\right)^{1/\alpha} + \left(\frac{w_l(\mathbf{s}_j)}{z(\mathbf{s}_j)}\right)^{1/\alpha}\right]^{\alpha}\right\}$. For more than two locations, we are also able to compute the exact likelihood when the number of locations is large but the number of events is small, as might be expected for very rare events (see Appendix A.2).

4 Quantifying spatial dependence

Assume that Z_1 and Z_2 are both GEV$(\beta, 1, 1)$ so that the probability of Y_i decreases to zero as β increases. A common measure of dependence between binary variables is Cohen's Kappa (Cohen, 1960),

$$\kappa(\beta) = \frac{P_A - P_E}{1 - P_E} \tag{7}$$

where P_A is the joint probability of agreement and P_E is the joint probability of agreement under an assumption of independence. For the spatial model, we get

$$\begin{aligned} P_A(\beta) &= 1 - 2\exp\left\{-\frac{1}{\beta}\right\} + 2\exp\left\{-\frac{\vartheta(\mathbf{s}_1, \mathbf{s}_2)}{\beta}\right\} \\ P_E(\beta) &= 1 - 2\exp\left\{-\frac{1}{\beta}\right\} + 2\exp\left\{-\frac{2}{\beta}\right\}, \end{aligned}$$

and

$$\kappa(\beta) = \frac{P_A(\beta) - P_E(\beta)}{1 - P_E(\beta)} = \frac{\exp\left\{-\frac{\vartheta(\mathbf{s}_1,\mathbf{s}_2)-1}{\beta}\right\} - \exp\left\{-\frac{1}{\beta}\right\}}{1 - \exp\left\{-\frac{1}{\beta}\right\}} \tag{8}$$

where $\vartheta(\mathbf{s}_i, \mathbf{s}_j) = \sum_{l=1}^{L}\left[w_l(\mathbf{s}_i)^{1/\alpha} + w_l(\mathbf{s}_j)^{1/\alpha}\right]^{\alpha}$ is the pairwise extremal coefficient given by Reich and Shaby (2012). To measure extremal dependence, let β go to ∞ so that events are increasingly more rare. Then,

$$\kappa = \lim_{\beta\to\infty} \kappa(\beta) = 2 - \vartheta(\mathbf{s}_1, \mathbf{s}_2) \tag{9}$$

which is the same as the χ statistic of Coles et al. (1999), a commonly used measure of extremal dependence.

5 Computation

For small K we can evaluate the likelihood directly. When K is large, we use MCMC methods with the random effects model to explore the posterior distribution. This is possible because the expression for the joint density, conditional on $A_1, \ldots, A_L$, is given by

$$P[Y(\mathbf{s}_1) = y(\mathbf{s}_1), \ldots, Y(\mathbf{s}_n) = y(\mathbf{s}_n)] = \prod_{i=1}^{n} \pi(\mathbf{s}_i)^{1-Y_i}[1 - \pi(\mathbf{s}_i)]^{Y_i}. \tag{10}$$

where $\pi(\mathbf{s}_i)$ is given in (3). The model parameters and random effects are updated using a combination of Metropolis Hastings (MH) and Hamiltonian Monte Carlo (HMC) update steps. To overcome challenges with evaluating the positive stable density, we follow Reich and Shaby (2012) and incorporate the auxiliary variable technique of Stephenson (2009).

6 Simulation study

For our simulation study, we generate $n_m = 50$ datasets under 6 different settings to explore the impact of sample size and misspecification of link function. We generate data assuming three possible types of underlying process. For each process, we consider two sample sizes $n_s = 650$ and $n_s = 1300$.

The first of these processes is a max-stable process that uses the GEV link described in (1) with knots on a 21×21 regularly spaced grid on $[0, 1] \times [0, 1]$. For this process, we set $\alpha = 0.3$, $\rho = 0.025$, $\xi = 0$ for idenfiability purposes, and β_0 is set for each dataset to give 5% rarity. We then set $Y(\mathbf{s}) = I[z(\mathbf{s}) > 0]$ where $I[\cdot]$ is an indicator function.

For the second process, we generate a latent variable from a spatial Gaussian process with a mean of

logit$(0.05) \approx -2.9444$ and an exponential covariance given by

$$\text{cov}(\mathbf{s}_1, \mathbf{s}_2) = \tau^2_{\text{Gau}} * \exp\left\{-\frac{||\mathbf{s}_1 - \mathbf{s}_2||}{\rho_{\text{Gau}}}\right\} \tag{11}$$

where $\tau_{\text{Gau}} = 10$ and $\rho_{\text{Gau}} = 0.05$. The mean of the Gaussian process is set to give approximately 5% rarity. Finally, we generate $Y(\mathbf{s}) \overset{ind}{\sim} \text{Bern}[\pi(\mathbf{s})]$ where $\pi(\mathbf{s}) = \exp\left\{\frac{z(\mathbf{s})}{1+z(\mathbf{s})}\right\}$

For the third process, we generate data using a hotspot method. For this process, we first generate hotspots throughout the space. Let n_{hs} be the number of hotspots in the space. Then $n_{\text{hs}} - 1 \sim \text{Poisson}(2)$. This generation scheme ensures that every dataset has at least one hotspot. We generate the hotspot locations $\mathbf{h}_1, , \mathbf{h}_{n_{\text{hs}}}$ Let $\mathcal{B}_\langle$ be a circle of radius of radius 0.08 around hotspot $h = 1, \ldots, n_{\text{hs}}$. We set $\text{P}[Y(\mathbf{s}_i) = 1] = 0.95$ for all $\mathbf{s}_i$ in $\mathcal{B}_\langle$, and $\text{P}[Y(\mathbf{s}_i)] = 0.01$ fr all $\mathbf{s}_i$ outside of $\mathcal{B}_\langle$. These settings are selected to give an average rate of close to 5% for each dataset.

For each dataset, we fit the model using three different methods, the proposed spatial GEV method, a spatial probit, and a spatial logistic model.

6.1 Spatial logistic and probit methods

Because logistic and probit methods represent two of the more common spatial techniques for binary data, we chose to compare our method to them. One way these methods differ from our proposed method is that they assume the underlying process is Gaussian. In this case, we assume that $Z(\mathbf{s})$ follows a Gaussian process with mean $\mathbf{X}(s)^T\boldsymbol{\beta}$ and exponential covariance function. The marginal distributions are given by

$$P(Y = 1) = \begin{cases} \frac{\exp[\mathbf{X}^T\boldsymbol{\beta} + \mathbf{W}\boldsymbol{\alpha}]}{1+\exp[\mathbf{X}^T\boldsymbol{\beta} + \mathbf{W}\boldsymbol{\alpha}]}, & \text{logistic} \\ \phi(\mathbf{X}^T\boldsymbol{\beta} + \mathbf{W}\boldsymbol{\alpha}), & \text{probit} \end{cases} \tag{12}$$

where $\boldsymbol{\alpha}$ are Gaussian random effects at the knot locations, and the $\mathbf{W}$ are basis functions to recreate the Gaussian process at all sites. We wrote our own code for the spatial probit model, but we use the `spGLM` function of `spBayes` to fit the spatial logistic model (Finley et al., 2015).

6.2 Cross validation

For each dataset, we fit the model using the n_s observations as a training set, and generate an additional 1,000 observations to use in validating the model's predictive power. Let $\mathbf{s}_j^*$ be the site for each observation in the validation set. To obtain the posterior predictive distribution, at each iteration of the MCMC, we generate a spatial field of zeros and ones at the validation locations. Then to obtain $\hat{P}[Y(\mathbf{s}_j^*) = 1]$, we take the average of the posterior distribution for $j = 1, \ldots, 1000$. We consider a few different metrics for comparing model performance. One score is the Brier scores (Gneiting and Raftery, 2007, BS). The Brier score for predicting an occurrence at site $\mathbf{s}$ is given by $\{I[Y(\mathbf{s}) = 1] - \hat{P}[Y(\mathbf{s}) = 1]\}^2$ where $I[Y(\mathbf{s}) = 1]$ is an indicator function indicating that an event occurred at site $\mathbf{s}$. We average the Brier scores over all test sites, and a lower score indicates a better fit.

We also consider the receiver operating characteristic (ROC) curve, precision recall curve, as well as the area under the ROC curve (AUROC) for the different methods and settings. The ROC and PRC curves are computed using the `ROCR` (Sing et al., 2005) package in `R` (R Core Team, 2016). We then average AUCs across all datasets for each method and setting to obtain a single AUC for each combination of method and setting.

6.3 Results

Needs updating

Table 1 gives the Brier scores and AUC for each of the methods. In Figure 1, for each setting we present

Table 1: Brier scores and AUROC for GEV, Probit, and Logistic methods.

	BS			AUROC		
	GEV	Probit	Logistic	GEV	Probit	Logistic
Setting 1						
Setting 2						
Setting 3						
Setting 4						
Setting 5						
Setting 6						

Figure 1: Vertically averaged ROC curves for each setting and method.

the a vertically averaged ROC curve for each method.

We analyzed the results for this simulation study using a Friedman test at $\alpha = 0.05$ to see if at least one method had a significantly different Brier score or AUC. For any setting that yielded a significant p-value, we conducted a Wilcoxon-Nemenyi-McDonald-Thompson test to see which of the methods had different results. The full results for the Wilcoxon-Nemenyi-McDonald-Thompson tests are given in Appendix A.3.

7 Data analysis

Needs updating

We compare our method to the spatial probit and logit for mapping the probability of the occurance of two plant species, *Tamarix ramosissima* for a 1-km^2 study region of PR China Smith et al. (2012). The Chinese Academy of Forestry conducted a full census of the area, and the true occupancy of the species are plotted in Figure 2. The region is split into 5-m $\times$ 5-m grid cells. *Tamarix ramosissima* can be found in approximately 2.84% of the grid cells. We subsample the original data using $n = 100$ initial locations for two different sampling design. The first is a two-stage spatially-adaptive cluster technique (CLU) taken from Pacifici et al. (2016). In this design, if an initial location is occupied, we also include the four rook neighbor (north, east, south, and west) sites in the sample. For the second design, we use a simple random

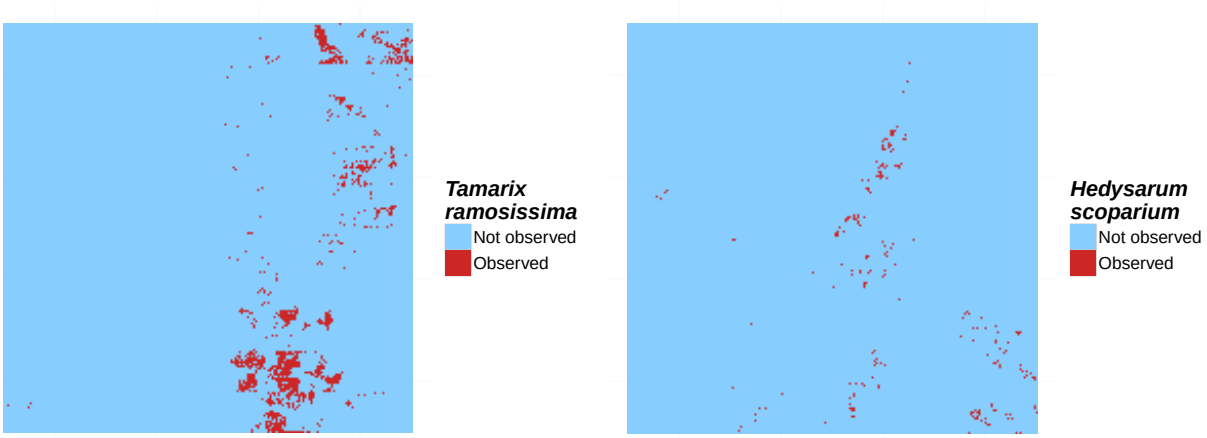

Figure 2: True occupancy of *Tamarix ramosissima* from a 1-km^2 study region of PR China.

sample (SRS) with the same number of sites included in the cluster sample.

For all models, we place knots on a 15×15 regularly spaced grid over the domain, and we also place knots at all sites where $Y(\mathbf{s}) = 1$. This knot arrangement is selected for two reasons. First, the regular grid provides a natural cutoff for the lower bound of the Uniform prior on ρ. This lower bound is important because if ρ is too small, relative to the knot placement, it is possible to end up with predictions at locations that are independent from all data points. There is a trade-off in selecting the number of knots to use for the random effects. If the knot spacing is too far apart, we risk a negative bias when estimating $P(Y = 1)$. One way to address this challenge is to provide a finer grid, but this can quickly become computationally burdensome. Furthermore, with a finer grid, we often end up increasing the resolution of the grid in areas that may not be important. Therefore, we choose to place additional knots at sites where $Y = 1$ as a balance between grid size and detail in the important areas.

For all models, we only include an intercept term β_0 in the model, and the prior for the intercept is $\beta_0 \sim \text{N}(0, 10)$. Additionally, for all models, the prior for the bandwidth is $\rho \sim \text{Unif}(\frac{1}{30}, 1)$. This lower bound is selected because it is half of the distance between the rook neighbors of the knots. For the GEV method, the prior for the spatial dependence parameter is $\alpha \sim \text{Beta}(2, 5)$. As with the simulation study, we select this prior because it gives greater weight to $\alpha < 0.5$, but also avoids values below 0.1 which can lead to

numerical problems. As with the simulation study, we fix $\xi = 0$ because we do not include any covariates.

For both the spatial probit and logistic models, the prior on the variance term for the random effects is IG$(0.1, 0.1)$ where IG$(\cdot)$ is an Inverse Gamma distribution. Both the spatial probit and logit models assume an exponetial covariance structure. For all models, we run the MCMC sampler for 25,000 iterations with a burn-in period of 20,000 iterations. Convergence is assessed through visual inspection of traceplots.

7.1 Results

8 Conclusions

Acknowledgments

A Appendices

A.1 Binary regression using the GEV link

Here, we provide a brief review of the the GEV link of Wang and Dey (2010). Let $Y_i \in \{0, 1\}, i = 1, \ldots, n$ be a collection of i.i.d. binary responses. It is assumed that $Y_i = I(z_i > 0)$ where $I(\cdot)$ is an indicator function, $z_i = [1 - \xi \mathbf{X}_i \boldsymbol{\beta}]^{1/\xi}$ is a latent variable following a GEV$(1, 1, 1)$ distribution, $\mathbf{X}_i$ is the associated p-vector of covariates with first element equal to one for the intercept, and $\boldsymbol{\beta}$ is a p-vector of regression coefficients. Then, $Y_i \overset{ind}{\sim}$ Bern(π_i) where $\pi_i = 1 - \exp\left(-\frac{1}{z_i}\right)$.

A.2 Derivation of the likelihood

We use the hierarchical max-stable spatial model given by Reich and Shaby (2012). If at each margin, $Z_i \sim$ GEV$(1, 1, 1)$, then $Z_i|\theta_i \overset{indep}{\sim}$ GEV$(\theta, \alpha\theta, \alpha)$. We reorder the data such that $Y_1 = \ldots = Y_K = 1$, and $Y_{K+1} = \ldots = Y_n = 0$. Then the joint likelihood conditional on the random effect θ is

$$
\begin{aligned}
P(Y_1 = y_1, \ldots, Y_n = y_n) &= \prod_{i \le K} \left\{ 1 - \exp\left[- \left(\frac{\theta_i}{z_i} \right)^{1/\alpha} \right] \right\} \prod_{i > K} \exp\left[- \left(\frac{\theta_i}{z_i} \right)^{1/\alpha} \right] \\
&= \exp\left[- \sum_{i=K+1}^{n} \left(\frac{\theta_i}{z_i} \right)^{1/\alpha} \right] - \exp\left[- \sum_{i=K+1}^{n} \left(\frac{\theta_i}{z_i} \right)^{1/\alpha} \right] \sum_{i=1}^{K} \exp\left[- \left(\frac{\theta_i}{z_i} \right)^{1/\alpha} \right] \\
&\quad + \exp\left[- \sum_{i=K+1}^{n} \left(\frac{\theta_i}{z_i} \right)^{1/\alpha} \right] \sum_{1 < i < j \le K} \left\{ \exp\left[- \left(\frac{\theta_i}{z_i} \right)^{1/\alpha} - \left(\frac{\theta_j}{z_j} \right)^{1/\alpha} \right] \right\} \\
&\quad + \cdots + (-1)^K \exp\left[- \sum_{i=1}^{n} \left(\frac{\theta_i}{z_i} \right)^{1/\alpha} \right] \qquad (13)
\end{aligned}
$$

Finally marginalizing over the random effect, we obtain

$$
\begin{aligned}
P(Y_1 = y_1, \ldots, Y_n = y_n) &= \int G(\mathbf{z}|\mathbf{A}) p(\mathbf{A}|\alpha) d\mathbf{A}. \\
&= \int \exp\left[- \sum_{i=K+1}^{n} \left(\frac{\theta_i}{z_i} \right)^{1/\alpha} \right] - \exp\left[- \sum_{i=K+1}^{n} \left(\frac{\theta_i}{z_i} \right)^{1/\alpha} \right] \sum_{i=1}^{K} \exp\left[- \left(\frac{\theta_i}{z_i} \right)^{1/\alpha} \right] \\
&\quad + \exp\left[- \sum_{i=K+1}^{n} \left(\frac{\theta_i}{z_i} \right)^{1/\alpha} \right] \sum_{1 < i < j \le K} \left\{ \exp\left[- \left(\frac{\theta_i}{z_i} \right)^{1/\alpha} - \left(\frac{\theta_j}{z_j} \right)^{1/\alpha} \right] \right\} \\
&\quad + \cdots + (-1)^K \exp\left[- \sum_{i=1}^{n} \left(\frac{\theta_i}{z_i} \right)^{1/\alpha} \right] p(\mathbf{A}|\alpha) d\mathbf{A}. \qquad (14)
\end{aligned}
$$

Consider the first term in the summation,

$$\int \exp\left\{-\sum_{i=K+1}^{n}\left(\frac{\theta_i}{z_i}\right)^{1/\alpha}\right\} p(\mathbf{A}|\alpha)d\mathbf{A} = \int \exp\left\{-\sum_{i=K+1}^{n}\left(\frac{\left[\sum_{l=1}^{L} A_l w_l(\mathbf{s}_i)^{1/\alpha}\right)^{\alpha}\right]^{1/\alpha}}{z_i}\right\} p(\mathbf{A}|\alpha)d\mathbf{A}$$

$$= \int \exp\left\{-\sum_{i=K+1}^{n}\sum_{l=1}^{L} A_l\left(\frac{w_l(\mathbf{s}_i)}{z_i}\right)^{1/\alpha}\right\} p(\mathbf{A}|\alpha)d\mathbf{A}$$

$$= \exp\left\{-\sum_{l=1}^{L}\left[\sum_{i=K+1}^{n}\left(\frac{w_l(\mathbf{s}_i)}{z_i}\right)^{1/\alpha}\right]^{\alpha}\right\}. \tag{15}$$

The remaining terms in equation (14) are straightforward to obtain, and after integrating out the random effect, the joint density for $K = 0, 1, 2$ is given by

$$P(Y_1 = y_1, \ldots, Y_n = y_n) = \begin{cases} G(\mathbf{z}) & K = 0 \\ G(\mathbf{z}_{(1)}) - G(\mathbf{z}) & K = 1 \\ G(\mathbf{z}_{(12)}) - G(\mathbf{z}_{(1)}) - G(\mathbf{z}_{(2)}) + G(\mathbf{z}) & K = 2 \end{cases} \tag{16}$$

where

$$G[\mathbf{z}_{(1)}] = P[Z(\mathbf{s}_2) < z(\mathbf{s}_2), \ldots, Z(\mathbf{s}_n) < z(\mathbf{s}_n)]$$

$$G[\mathbf{z}_{(2)}] = P[Z(\mathbf{s}_1) < z(\mathbf{s}_1), Z(\mathbf{s}_3) < z(\mathbf{s}_3), \ldots, Z(\mathbf{s}_n) < z(\mathbf{s}_n)]$$

$$G[\mathbf{z}_{(12)}] = P[Z(\mathbf{s}_3) < z(\mathbf{s}_3), \ldots, Z(\mathbf{s}_n) < z(\mathbf{s}_n)].$$

Similar expressions can be derived for all K, but become cumbersome for large K.

A.3 Simulation study pairwise difference results

Needs updating

The following tables show the methods that have significantly different Brier scores when using a Wilcoxon-Nemenyi-McDonald-Thompson test. In each column, different letters signify that the methods have significantly different Brier scores.

Table 2: Pairwise BS comparisons

	Setting 1	Setting 2	Setting 3	Setting 4	Setting 5	Setting 6
Method 1	A	A	A	C	B	B
Method 2	A B	B	A	B	A	A
Method 3	B	B	A	A	A B	A

References

Cohen, J. (1960) A Coefficient of Agreement for Nominal Scales. *Educational and Psychological Measurement*, **20**, 37–46.

Coles, S., Heffernan, J. and Tawn, J. (1999) Dependence Measures for Extreme Value Analyses. *Extremes*, **2**, 339–365.

Finley, A. O., Banerjee, S. and Gelfand, A. E. (2015) spBayes for Large Univariate and Multivariate Point-Referenced Spatio-Temporal Data Models. *Journal of Statistical Software*, **63**.

Genton, M. G., Ma, Y. and Sang, H. (2011) On the likelihood function of Gaussian max-stable processes. *Biometrika*, **98**, 481–488.

Gneiting, T. and Raftery, A. E. (2007) Strictly Proper Scoring Rules, Prediction, and Estimation. *Journal of the American Statistical Association*, **102**, 359–378.

de Haan, L. (1984) A Spectral Representation for Max-stable Processes. *The Annals of Probability*, **12**, 1194–1204.

Heagerty, P. and Lele, S. (1998) A Composite Likelihood Approach to Binary Spatial Data. *Journal of the American Statistical Association*, **1459**, 1099–1111.

Huser, R. and Davison, A. C. (2014) Space-time modelling of extreme events. *Journal of the Royal Statistical Society: Series B (Statistical Methodology)*, **76**, 439–461.

Pacifici, K., Reich, B. J., Dorazio, R. M. and Conroy, M. J. (2016) Occupancy estimation for rare species using a spatially-adaptive sampling design. *Methods in Ecology and Evolution*, **7**, 285–293.

Padoan, S. A., Ribatet, M. and Sisson, S. A. (2010) Likelihood-Based Inference for Max-Stable Processes. *Journal of the American Statistical Association*, **105**, 263–277.

R Core Team (2016) *R: A Language and Environment for Statistical Computing*. R Foundation for Statistical Computing, Vienna, Austria. URL`https://www.R-project.org/`.

Reich, B. J. and Shaby, B. A. (2012) A hierarchical max-stable spatial model for extreme precipitation. *The Annals of Applied Statistics*, **6**, 1430–1451.

Sing, T., Sander, O., Beerenwinkel, N. and Lengauer, T. (2005) ROCR: visualizing classifier performance in R. *Bioinformatics*, **21**, 3940–3941.

Smith, D. R., Yuancai, L., Walter, C. A. and Young, J. A. (2012) Incorporating predicted species distribution in adaptive and conventional sampling designs. In *Design and Analysis of Long-term Ecological Monitoring Studies* (eds. R. A. Gitzen, J. J. Millspaugh, A. B. Cooper and D. S. Licht), chap. 17, 381–396. Cambridge University Press.

Stephenson, A. G. (2009) High-Dimensional Parametric Modelling of Multivariate Extreme Events. *Australian & New Zealand Journal of Statistics*, **51**, 77–88.

Tawn, J. A. (1990) Modelling multivariate extreme value distributions. *Biometrika*, **77**, 245–253.

Thibaud, E. and Opitz, T. (2015) Efficient inference and simulation for elliptical Pareto processes. *Biometrika*, **102**, 855–870.

Wadsworth, J. L. and Tawn, J. A. (2014) Efficient inference for spatial extreme value processes associated to log-Gaussian random functions. *Biometrika*, **101**, 1–15.

Wang, X. and Dey, D. K. (2010) Generalized extreme value regression for binary response data: An application to B2B electronic payments system adoption. *The Annals of Applied Statistics*, **4**, 2000–2023.